The Role of Polymer Architecture in Strengthening Polymer−Polymer Interfaces: A Comparison of Graft, Block, and Random Copolymers Containing Hydrogen-Bonding Moieties

Brian D. Edgecombe, Jason A. Stein, and Jean M. J. Fréchet*

Department of Chemistry, Baker Laboratory, Cornell University, Ithaca, New York 14853-1301, and Department of Chemistry, University of California, Berkeley, California 94720-1460

Zhihua Xu and Edward J. Kramer†

Department of Materials Science and Engineering and the Materials Science Center, Cornell University, Ithaca, New York 14853-1301

Received June 10, 1997

ABSTRACT: A series of styrene-d_8/4-hydroxystyrene graft and block copolymers has been prepared by "living" radical and anionic techniques for use in interfacial strengthening studies at the polystyrene/poly(2-vinylpyridine), PS/PVP, interface. The following copolymers in which A and B segments represent poly(styrene-d_8) and poly(4-hydroxystyrene), respectively, have been prepared: poly(A-*graft*-B), poly(B-*graft*-A), poly(B-*block*-A-*block*-B), poly(A-*block*-B-*block*-A-*block*-B-*block*-A). The poly(4-hydroxystyrene) segments were obtained by "living" radical polymerization of 4-acetoxystyrene or anionic polymerization of 4-methoxystyrene, followed by conversion to the phenolic derivative. In general, the amphiphilic copolymers when placed at the PS/PVP interface acted as interfacial reinforcers but were susceptible to the formation of microphases such as lamellae or micelles, and therefore the measured fracture toughness depended on both the copolymer/homopolymer interfacial strength and the toughness of the copolymer phase structure itself. The pentablock copolymer showed better strengthening behavior than the triblock copolymer especially at very low areal chain density. The strengthening ability of the graft copolymers was found to depend on the lengths of the polystyrene, PS, and poly(4-hydroxystyrene), PS(OH), segments. In both graft and block copolymers the PS(OH) segments were found to resist pull-out from the bulk PVP even at low degrees of polymerization ($N_{PS(OH)} = 29$). The H-bonding interaction between the phenolic and pyridyl groups combined with the severe immiscibility of poly(4-hydroxystyrene) and polystyrene is the most likely cause for pull-out resistance.

Introduction

Copolymers at the interface between immiscible polymers are known to have significant effects on interfacial properties when the appropriate copolymer structure is employed. For example, block,[1−8] random,[9−13] and graft[14−17] copolymers have been studied for their ability to toughen model interfaces or polymer blends. Depending on the copolymer architecture and the nature of the copolymer−polymer interaction, different degrees of toughening can be achieved. The majority of interfacial toughening investigations have relied on nonspecific interactions as the driving force for copolymer segregation and reinforcement via entanglement. Typically in block copolymer studies A−B block copolymers are used to strengthen the interface between homopolymers A and B. For strengthening to occur, the blocks of the copolymer must be long enough to allow chain entanglement with the respective bulk homopolymer. However, long symmetric diblock copolymers tend to form lamellae at the interface.[4] Since the interfaces between the sub-lamellae within the copolymer layer are weak, the degree to which diblock copolymers can reinforce the interface is limited. In contrast long triblock copolymers (ABA)[7] are very effective as interfacial reinforcers despite their tendency to form cylindrical micelles. The interfacial activity of A−B random copolymers which do not form phase domains has also been studied at A/B interfaces. In the polystyrene/poly(2-vinylpyridine), PS/PVP, system random copolymers with nearly a 50:50 composition were found to be surprisingly effective at strengthening the interface at very low areal chain densities.[10]

Following early work on the use of enthalpically favorable H-bonding interactions to compatibilize polymers[18] or form extended liquid-crystalline mesophases,[19] we have recently reported the effect of H-bonding interactions at the polymer−polymer interface.[20] We have extended this study to the strengthening of the PS/PVP interfaces by designing a variety of copolymers capable of H-bonding interactions. It has been demonstrated previously that copolymers capable of multiple interactions across the interface can entangle with each side of the interface and act as effective reinforcers.[9,10] Therefore, random, block, and graft copolymers with functional groups capable of hydrogen bonding (Chart 1 in which F denotes a H-bonding functionality) have been selected as candidates for interfacial reinforcers because of their potential for forming multiple anchoring crossover points at the PS/PVP phase boundary. These copolymers are representative of the many different architectures that may be designed to maximize interfacial strengthening through the formation of hydrogen bonds at the interface between immiscible components.

For example, we have recently reported the surprising strengthening effects of a series of random copolymers

* Author to whom all correspondence should be addressed at the Department of Chemistry, University of California, Berkeley, CA 94720-1460.

† Current address: Department of Materials, University of California at Santa Barbara, Santa Barbara, CA 93106.

S0024-9297(97)00832-2 CCC: $15.00
Published on Web 02/04/1998

Chart 1

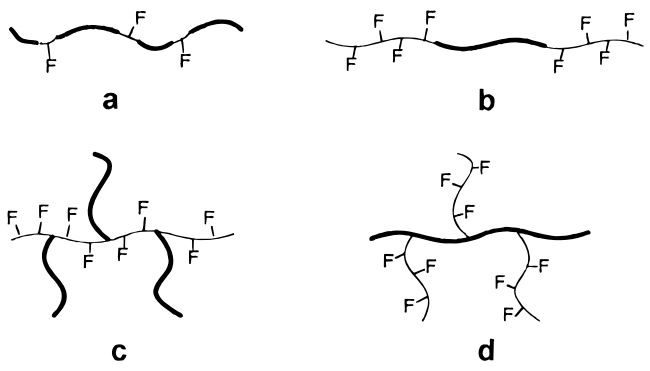

(Chart 1, type **a**), poly(styrene-*co*-4-hydroxystyrene), each with a different composition, at the PS/PVP interface.[21] Remarkably high interfacial fracture toughness values were obtained when random copolymers with low incorporation of 4-hydroxystyrene (molar fraction $f < 0.05$) were placed at the interface. The sensitivity of the strengthening behavior to composition was attributed to the effective "repulsion" between the covalently bonded styrene and 4-hydroxystyrene units combined with the attractive interaction available at the interface between the 4-hydroxystyrene and vinylpyridine units. The large driving force for segregation of the 4-hydroxystyrene units from the styrene units is at least in part the result of the strong self-association of the phenols via hydrogen bonding. High fracture toughness is afforded by a layer of random copolymer of the appropriate composition as a consequence of its ability to simultaneously form strong PS/copolymer and PVP/copolymer interfaces.

Because such a pronounced effect originating from a very low concentration of active groups was unexpected, we decided to explore the effect of copolymers with similar functionality but different architectures on interfacial strengthening. Block copolymers (Chart 1, type **b**) are expected to cross the interface multiple times depending on the number of incorporated blocks (e.g., triblock, pentablock). Graft architectures allow two distinct placements of interacting groups: as part of either the side chains (Chart 1, type **c**) or the main chain (Chart 1, type **d**) of the grafted structure. This feature permits comparisons to be made for the determination of the effect of copolymer architecture on interfacial strengthening.

Experimental Section

Materials. Polystyrene, PS ($M_w = 280\,000$, $M_w/M_n = 2.1$), and poly(2-vinylpyridine), PVP ($M_w = 200\,000$ $M_w/M_n = 2.4$), were purchased from Aldrich and Polysciences, respectively, and were used as received. Styrene-d_8 (97%) was obtained from Cambridge Isotopes. The monomers were simply distilled before use in polymerizations. α,α′-Dichloro-*p*-xylene (Aldrich) was recrystallized from hexane. Ethyl valerate, *tert*-pentanol, and xylenes were distilled from CaH_2. Vinylbenzyl chloride (3- and 4-mixed isomer) was passed through a plug of activated alumina prior to use. All other reagents were used as received. Degassing of solutions was carried out when noted via a freeze−pump−thaw cycle (4×). All reactions were carried out under a nitrogen purge unless otherwise stated.

Methods. The molecular weights of the polymers were determined by SEC using a liquid chromatograph equipped with a differential refractometer (refractoMonitor IV, Milton Roy). Tetrahydrofuran (THF) at 40 °C was used as the mobile phase at a nominal flow rate of 1 mL/min. Four 5 mm PL Gel columns with porosities of 100, 500, and 1000 Å and Mixed C were used to achieve separations. The system was calibrated with 20 monodisperse polystyrene standards. Infrared spectra were recorded on a Nicolet IR/44 spectrophotometer using a suspension of the compounds in a potassium bromide film. NMR spectra were recorded on a Bruker AF300 (300 MHz) spectrometer using the solvent proton signal as the internal standard. Glass transition temperatures were measured using a Seiko DSC 220C differential scanning calorimeter and a Seiko SSC/5200 thermal analysis station. Heating rates were 20 K/min after an initial annealing run. The glass transition temperature was recorded as the midpoint of the inflection tangent.

Poly(styrene-*co*-4-methylstyrene) (1b). The copolymerization was carried out in the bulk with styrene-d_8 (4.7 g), 4-methylstyrene (14 mg), and dicumyl peroxide (14 mg) at 105 °C for 12 h. The resulting copolymer was dissolved in THF, precipitated into excess methanol, filtered, and dried in vacuo. Yield: 4.48 g (95%). ^{1}H NMR (CD_2Cl_2): δ 7.2−6.4 (broad, Ar***H***), 2.4−2.2 (broad, Ar−C***H***$_3$), 2.0−1.2 (broad, −C***H***$_2$−C***H***(Ar)−). NMR shows 0.5 mol % incorporation of 4-methylstyrene units calculated from the comparison of the integration of the methyl resonances and the aromatic resonances. SEC: $M_n = 468\,000$, $M_w/M_n = 1.73$. See Table 1 for results of other copolymerization (**1a**).

1-Phenyl-1-(2′,2′,6′,6′-tetramethyl-1′-piperidinyloxy)-ethane. This compound was prepared as described by Hawker et al.[22] Yield after recrystallization: 40%. ^{1}H NMR and ^{13}C NMR spectra are consistent with published data.[22]

Poly(styrene-*co*-4-methylstyrene) (1c). A solution of 1-phenyl-1-(2′,2′,6′,6′-tetramethyl-1′-piperidinyloxy)ethane (8 mg) in styrene-d_8 (5.0 g) and 4-methylstyrene (53 mg) was degassed, backfilled with argon, and then heated to 125 °C for 24 h. The resulting copolymer was dissolved in THF, precipitated into excess methanol, filtered, and dried in vacuo. Yield: 4.64 g (92%). ^{1}H NMR (CD_2Cl_2): δ 7.2−6.4 (broad, Ar***H***), 2.4−2.2 (broad, Ar−C***H***$_3$), 2.0−1.2 (broad, −C***H***$_2$−C***H***(Ar)−). NMR shows 3 mol % incorporation of 4-methylstyrene units calculated from the comparison of the integration of the methyl resonances and the aromatic resonances. SEC: $M_n = 90\,300$, $M_w/M_n = 1.32$.

Polymer Metalation and Graft Polymerization. Metalations and anionic polymerizations were performed under an atmosphere of argon in flasks equipped with three-way stopcocks. All purified reagents were stored under argon in flasks equipped with three-way stopcocks or Teflon stopcocks. Glassware was flame-dried under vacuum and backfilled with argon immediately prior to use. Reagent transfer was performed carefully using gas-tight syringes and cannulae with rubber septa. A THF still was prepared with THF, previously distilled from lithium aluminum hydride, and Na/anthracene. 4-Methoxystyrene was distilled under vacuum from CaH_2 and stored under argon for subsequent use. Prior to each polymerization, 4-methoxystyrene was stirred with dibutylmagnesium for 30 min at room temperature under argon and then vacuum transferred. Methanol and chlorotrimethylsilane were distilled from CaH_2 under argon, degassed, and stored under argon. *sec*-Butyllithium solutions in cyclohexane were used as received from Aldrich or diluted with dry cyclohexane, freshly distilled from Na/benzophenone/tetraglyme, to the desired concentration. The concentration of *sec*-butyllithium was determined by titrating the *sec*-butyllithium solution in the presence of 1,10-phenanthroline with a standardized solution of *tert*-pentanol in xylenes.

Potassium *tert*-Pentoxide (t-PeOK). In a glovebox freshly cut potassium (8.10 g) was added to a solution of *tert*-pentanol (13.0 mL) in dry cyclohexane (450 mL). The solution was warmed slowly and maintained at reflux until all the potassium was consumed and the pentoxide was dissolved (12 h). For the determination of the solution concentration, an aliquot of the solution (1 mL) was added to water/2-propanol (1:1 v/v) and the base was titrated with a standardized solution of aqueous HCl using phenolphthalein as the end-point indicator (0.375 M potassium *tert*-pentoxide in cyclohexane).

Poly(styrene-*graft*-4-methoxystyrene) (4c). Poly(styrene-*co*-4-methylstyrene) (1.0 g, $M_w = 105\,000$, $M_w/M_n = 1.17$) was

Table 1. Characterization of Random and Graft Copolymers Prepared via Metalation with a Superbase

copolymer	M_n[d] ($\times 10^3$)	M_w/M_n	f_{MS}[a]	SB/MS[b]	f_K[c]	P_n main chain	graft points per chain[c]	P_n[d] graft	$M_{n,calc}$[e] ($\times 10^3$)
1a	44.4	1.51	0.027	0.88	0.019	425			
4a	47.4	1.55				425	8	6	50.9
1b	468	1.73	0.005	1.0	0.002	4480			
4b	461	1.79				4480	9	18	497
1c	90.3	1.17	0.030	0.22	0.004	864			
4c	116	1.32				864	3.5	75	113

[a] Determined from NMR data. [b] Molar ratio of superbase/4-methylstyrene units. [c] Metalation efficiency determined from NMR data of silylated polymer, **3**. [d] Calculated from NMR comparison of **1** and **4** using calculated number of graft points. [e] Calculated from the SEC data of **1** and the NMR data of **4**.

transferred into a flask in a glovebox. A solution of the copolymer was prepared by adding freshly distilled THF (50 mL) to the flask via a cannula. The solution was cooled to −75 °C and titrated to dryness by dropwise addition of *sec*-butyllithium (1.2 M in cyclohexane) until a light green color was observed. The solution was then allowed to warm to room temperature, during which the color faded due to the decomposition of the residual alkyllithium in the presence of THF. After cooling the solution again to −75 °C, the superbase was generated in situ via addition of t-PeOK (0.79 mL, 0.375 M in cyclohexane), followed by *sec*-butyllithium (0.72 mL, 0.082 M in cyclohexane). A red color was observed which indicated that metalation of the polymer had occurred. After stirring at −75 °C for 45 min, an aliquot (3 mL) was removed and quenched with chlorotrimethylsilane. Freshly distilled 4-methoxystyrene (0.32 mL) was added slowly dropwise to the vigorously stirred metalated polymer solution, leading to an increase in the red color intensity. The polymerization was terminated by addition of degassed methanol. The polymer was precipitated into excess methanol, filtered, and dried in vacuo. ^{1}H NMR (CD_2Cl_2): δ 7.2−7.0 (broad, Ar***H***), 7.0−6.2 (broad, Ar***H***), 3.9−3.7 (broad, Ar−OC***H***$_3$), 2.4−2.2 (broad, Ar−C***H***$_3$), 2.2−1.2 (broad, −C***H***$_2$−C***H***(Ar)−). NMR shows 21 mol % incorporation of 4-methoxystyrene units calculated from the integration of the methoxy resonances and the aromatic resonances. SEC: M_n = 116 000, M_w/M_n = 1.32. See Table 1 for results of other graft copolymerizations (**4a,b**).

Poly(styrene-*graft*-4-hydroxystyrene) (5c). Boron tribromide (1.36 g, 3.0 equiv with respect to methoxy groups) was added via a gas-tight syringe to a solution of poly(styrene-*graft*-4-methoxystyrene) in dichloromethane (1.0 g in 20 mL) cooled in a dry ice/ethanol bath. The reaction was allowed to slowly come to room temperature (12 h). After cooling the solution again to −75 °C, the reaction was quenched by slow addition of methanol/water (1:1 v/v). Pyridine was added to dissolve the copolymer and neutralize any residual acid. After removing dichloromethane by evaporation, the polymer was precipitated from a pyridine solution into excess water, filtered, and dried in vacuo at 60 °C. ^{1}H NMR (DMF-d_7): δ 9.4−9.0 (broad, Ar−OH), 7.2−7.0 (broad, Ar***H***), 7.0−6.2 (broad, Ar***H***), 2.4−2.2 (broad, Ar−C***H***$_3$), 2.2−1.2 (broad, −C***H***$_2$−C***H***(Ar)−). DSC: T_{g1} = 105 °C; T_{g2} = 194 °C. **5a** and **5b** exhibited T_g = 106 °C.

Poly(styrene-*graft*-4-acetoxystyrene). Acetic anhydride (0.280 g) was added to a solution of graft copolymer **5c** (0.304 g in 10 mL of THF/2 mL of pyridine) cooled to 0 °C. The solution was slowly brought to room temperature (2 h). After 12 h the excess acetic anhydride was quenched by addition of 5 mL of a pyridine/water solution (4:1 v/v) and the THF was removed via evaporation. The polymer was precipitated into excess water/methanol (1:1 v/v), filtered, and dried in vacuo at 40 °C. The FTIR spectrum shows a strong absorption at 1763 cm^{-1} corresponding to the carbonyl stretch and a nearly complete loss of the hydroxyl absorption at 3300−3500 cm^{-1}. SEC: M_n = 113 100, M_w/M_n = 1.45.

Poly(4-acetoxystyrene-*co*-vinylbenzyl chloride) (6). A solution of 1-phenyl-1-(2′,2′,6′,6′-tetramethyl-1′-piperidinyloxy-)ethane (41 mg, 1.0 equiv) in 4-acetoxystyrene (5.0 g, 196 equiv) and vinylbenzyl chloride (96 mg, 4 equiv) was degassed, backfilled with argon, then heated to 125 °C for 24 h. The resulting polymer was dissolved in THF, precipitated into excess methanol, filtered, and dried in vacuo. Yield: 3.56 g (70%). ^{1}H NMR ($CDCl_3$): δ 7.0−6.4 (broad, Ar***H***), 4.6−4.3 (broad, Ar−C***H***$_2$−Cl), 2.5−2.1 (broad, Ar−O−C(O)−C***H***$_3$), 2.2−1.2 (broad, −C***H***$_2$−C***H***(Ar)−). NMR shows 1.7 mol % incorporation of vinylbenzyl chloride units calculated from comparison of the integration of the chloromethyl resonances and the acetate resonances. SEC: M_n = 19 700, M_w/M_n = 1.14.

Table 2. Characterization of Graft Copolymers Prepared via ATRP

copolymer	f_{Cl}[a]	arms/ chain[b]	M_n ($\times 10^3$)	PD	$M_{n,calc}$[c] ($\times 10^3$)
6	0.017		19.7	1.14	
7a		2.4	76.6	1.63	78.8
7b		2.4	87.4	1.77	111

[a] Molar ratio of vinylbenzyl chloride units in polymer **6**, determined from ^{1}H NMR data. [b] Calculated from NMR and SEC data of **6**. [c] Calculated from the NMR data.

Poly(4-acetoxystyrene-*graft*-styrene) (7a). Polymeric initiator **6** (1.0 g, 1.0 equiv of benzyl chloride) was combined with copper(I) chloride (12 mg, 1.0 equiv), 2,2′-dipyridine (42 mg, 2.2 equiv), styrene (5.08 g, 400 equiv), and ethyl valerate (0.5 mL) as solvent/plasticizer in a sealable vessel. The solution was degassed, backfilled with argon, sealed, and heated to 110 °C for 24 h. Within 30 s of heating, the initially green mixture turned dark reddish brown and became more homogeneous. After 12 h the vessel was cooled and opened and the polymer was diluted in THF leading again to a green mixture. The heterogeneous polymer/catalyst mixture was passed through a plug of activated alumina to remove the insoluble copper salts, concentrated via evaporation, precipitated into excess methanol, filtered, and dried in vacuo at 50 °C. Monomer conversion: 64%. ^{1}H NMR (CD_2Cl_2): δ 7.2−6.2 (broad, Ar***H***), 2.4−2.2 (broad, Ar−O−C(O)−C***H***$_3$), 2.2−1.2 (broad, −C***H***$_2$−C***H***(Ar)−). NMR shows 73 mol % incorporation of styrene-d_8 units calculated from the comparison of the integration of the acetate resonances and the aromatic resonances. SEC: M_n = 76 600, M_w/M_n = 1.63. See Table 2 for results of the other copolymerization (**7b**).

Poly(4-hydroxystyrene-*graft*-styrene) (8a). Tetrabutylammonium hydroxide (1.65 g, 40 wt % in water) was added to a pyridine solution of **7a** (1.0 g/20 mL) at room temperature. The reaction was quenched after 1 h by the addition of dry ice. The polymer was precipitated from a pyridine solution into excess water/methanol (1:1 v/v). The polymer was filtered and dried in vacuo at 60 °C for 24 h. Yield: quantitative. The FTIR spectrum shows complete loss of carbonyl absorption (1765 cm^{-1}) and the appearance of a broad −OH absorption (3300−3500 cm^{-1}). DSC: T_g = 105 °C.

Poly(styrene-d_8) (9a). In a typical polymerization, styrene-d_8 (3.23 g, 290 equiv) was combined with α,α′-dichloro-*p*-xylene (17 mg, 1 equiv), CuCl (20 mg, 2.0 equiv), 2,2′-dipyridine (69 mg, 4.4 equiv), and ethyl valerate (1 mL) as solvent/plasticizer in a sealable reaction vessel. The heterogeneous solution was degassed, backfilled with argon, and placed in a bath at 125 °C. The workup was the same as that for **7a**. Yield: 2.84 g (87%). ^{1}H NMR (CD_2Cl_2): δ 7.2−6.2 (broad, Ar***H***), 2.2−1.2 (broad, −C***H***$_2$−C***H***(Ar)−). SEC: M_n = 26 100, M_w/M_n = 1.22.

Poly(4-acetoxystyrene-*block*-styrene-d_8-*block*-4-acetoxystyrene) (10a). Polymeric initiator, **9a** (2.0 g, 1.0 equiv),

was combined with CuCl (16 mg, 2.0 equiv), 2,2′-dipyridine (61 mg, 5.0 equiv), 4-acetoxystyrene (1.85 g, 150 equiv), and ethyl valerate (1 mL) in a sealable reaction vessel. Solution was degassed, backfilled with argon, and heated to 125 °C for 24 h. Polymer workup was as described for **7a**. Yield: 2.92 g. Conversion: 50%. ^{1}H NMR (CD_2Cl_2): δ 7.2−6.2 (broad, Ar***H***), 2.4−2.2 (broad, Ar−O−C(O)−C***H***$_3$), 2.2−1.2 (broad, −C***H***$_2$−C***H***(Ar)−). NMR shows 19 mol % incorporation of 4-acetoxystyrene units calculated from the comparison of the integration of the acetate resonances and the aromatic resonances. SEC: M_n = 35 500, M_w/M_n = 1.27.

Poly(styrene-*d*$_8$-*block*-4-acetoxystyrene-*block*-styrene-*d*$_8$-*block*-4-acetoxystyrene-*block*-styrene-*d*$_8$) (12a). Polymeric initiator **10a** (0.53 g, 1.0 equiv) was combined with CuCl (7 mg, 3.4 equiv), 2,2′-dipyridine (21 mg, 6.6 equiv), styrene-d_8 (1.58 g, 718 equiv), and ethyl valerate (0.5 mL) in a sealable reaction vessel. Solution was degassed, backfilled with argon, and heated to 125 °C for 24 h. Polymer workup was as described for **7a**. Yield: 2.07 g. Conversion: 90%. ^{1}H NMR (CD_2Cl_2): δ 7.2−6.2 (broad, Ar***H***), 2.4−2.2 (broad, Ar−O−C(O)−C***H***$_3$), 2.2−1.2 (broad, −C***H***$_2$−C***H***(Ar)−). NMR shows 6 mol % incorporation of 4-acetoxystyrene units calculated from the comparison of the integration of the acetate resonances and the aromatic resonances. SEC: M_n = 108 900, M_w/M_n = 2.31.

Poly(styrene-*d*$_8$-*block*-4-hydroxystyrene-*block*-styrene-*d*$_8$-*block*-4-hydroxystyrene-*block*-styrene-*d*$_8$) (13a). Deprotection of **12a** was carried out as described for **8**. Yield: quantitative. The FTIR spectrum shows complete loss of carbonyl absorption (1765 cm^{-1}) and the appearance of a broad −OH absorption (3300−3500 cm^{-1}). DSC: T_g = 105 °C.

Poly(4-hydroxystyrene-*block*-styrene-*d*$_8$-*block*-4-hydroxystyrene) (11). This was prepared by deprotection of **10a** as described above for the preparation of **13a**.

Preparation of Samples for Fracture Toughness Measurements. For the preparation of the fracture toughness samples, PS and PVP plates were made by compression molding. The PS plate (2.3 mm) was made thicker than the PVP plate (1.7 mm) for reasons described below. A film of the copolymer was spun-cast from propyl acetate onto the optically smooth surface of the PVP plate. Since propyl acetate is a poor solvent for PVP, effects from the swelling of the PVP surface are expected to be small. The residual solvent was removed by heating the coated plate in a vacuum oven at 80 °C for 2 h. This plate was then welded to a PS plate at 160 °C for 2 h to form a layered assembly of PS/copolymer/PVP. This annealing step promotes diffusion of the copolymer into the respective homopolymers to form chain entanglements. The sample was then cut into strips with a diamond saw for the subsequent fracture toughness measurements. The dimensions of the strips were 50 mm long × 8.7 mm wide × 4.0 mm thick.

Fracture Toughness Measurements. The fracture toughness of the phase boundary, G_C, which is defined as the critical energy release rate of an interfacial crack, was measured using the asymmetric double-cantilever beam method (ADCB). The measurement was performed by inserting a single-edge razor blade at the phase boundary and pushing it at a constant rate of 3×10^{-6} m/s using a servo-controlled motor drive at room temperature. The steady-state value of the crack length, a, along the phase boundary ahead of the razor blade was measured at regular time intervals. The fracture toughness G_C, which is proportional to a^{-4}, was calculated[2] using these values of a. The error bars reported for G_C represent the standard deviation obtained from at least 10 measurements of the crack length. More details about the ADCB fracture test can found elsewhere.[1,2,23,24] Interfacial fracture toughness measurements were carried out using PS and PVP plates of different thicknesses which is necessary to produce a mechanical phase angle, $\psi \approx -6$. As shown by Xiao et al.,[25] the effect of shear stresses developing ahead of the crack on the measured toughness is minimized at $\psi \approx -6$ with the described geometry.

The use of deuterium-labeled copolymers in this study allowed for the determination of the role of the copolymer in the failure mechanism. After the fracture toughness measurement, the fracture surfaces of each test specimen were examined with forward recoil spectrometry (FRES)[2,26] to determine the amounts of deuterium from the residual copolymer. Using these data for each specimen, we calculated the apparent thickness and areal chain density of random copolymer on both PS (t_{PS} and Σ_{PS}, respectively) and PVP (t_{PVP} and Σ_{PVP}, respectively) sides. The total areal chain density, Σ, and thickness, t, of the copolymer were calculated by summing these two measurements; i.e., $\Sigma = \Sigma_{PS} + \Sigma_{PVP}$; $t = t_{PS} + t_{PVP}$. The fraction of copolymer remaining on each surface was also calculated from these values in order to evaluate the fracture mechanism.

The fracture study results are compared in the discussion below by plotting both fracture toughness and the fraction of ^{2}H on the PS side after fracture (Σ_{PS}/Σ) as functions of the amount of copolymer placed at the interface (copolymer layer thickness, t, and areal chain density, Σ). The solid line is our qualitative interpretation of the data trend. In the absence of copolymer the fracture toughness of the phase boundary is approximately 2 J/m^2.

Scheme 1

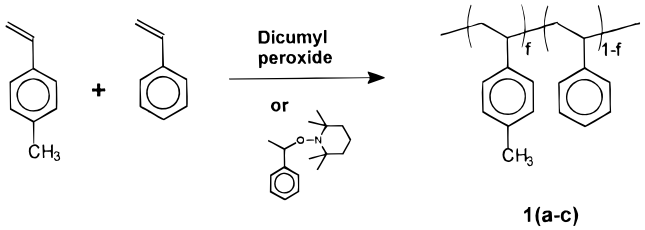

Results and Discussion

Synthesis of Graft Copolymers. While the preparation of functionalized block copolymers with well-defined molecular weights has been demonstrated in the literature, synthetic routes yielding functionalized graft copolymers of relatively narrow molecular weight distribution are not as common. Useful synthetic approaches to the preparation of graft copolymers include (i) copolymerizing a macromonomer with a monomer, (ii) reacting telechelic polymers with polymers bearing reactive groups throughout their main chain, and (iii) polymerizing a monomer from a polymer with multiple initiating sites located throughout its main chain. For the preparation of well-defined graft copolymers, a living polymerization mechanism must also be involved. In general, approach i is carried out by conventional radical polymerization, yielding graft copolymers with broad MW distributions, while approach ii often produces impure products due to the presence of unreacted homopolymer. To maintain control over grafting efficiency and graft arm length without necessitating laborious purifications, we have chosen to use the third synthetic approach. Using both "living" radical and anionic polymerization techniques, we have prepared novel graft copolymers with functionalized segments: poly(4-hydroxystyrene-*graft*-styrene) (Chart 1, type **c**) and poly(styrene-*graft*-4-hydroxystyrene) (Chart 1, type **d**). In the synthesis of both graft copolymers we use a random copolymer, prepared by "living" or standard free-radical techniques, that contains multiple activated sites along its main chain which can initiate the graft polymerization of an appropriately chosen monomer.

Metalation of Random Copolymers with Superbase. The linear random copolymers used as starting materials were prepared (Scheme 1) with varying molecular weights and molar ratios of 4-methylstyrene with respect to styrene in order to (i) obtain graft

Scheme 2

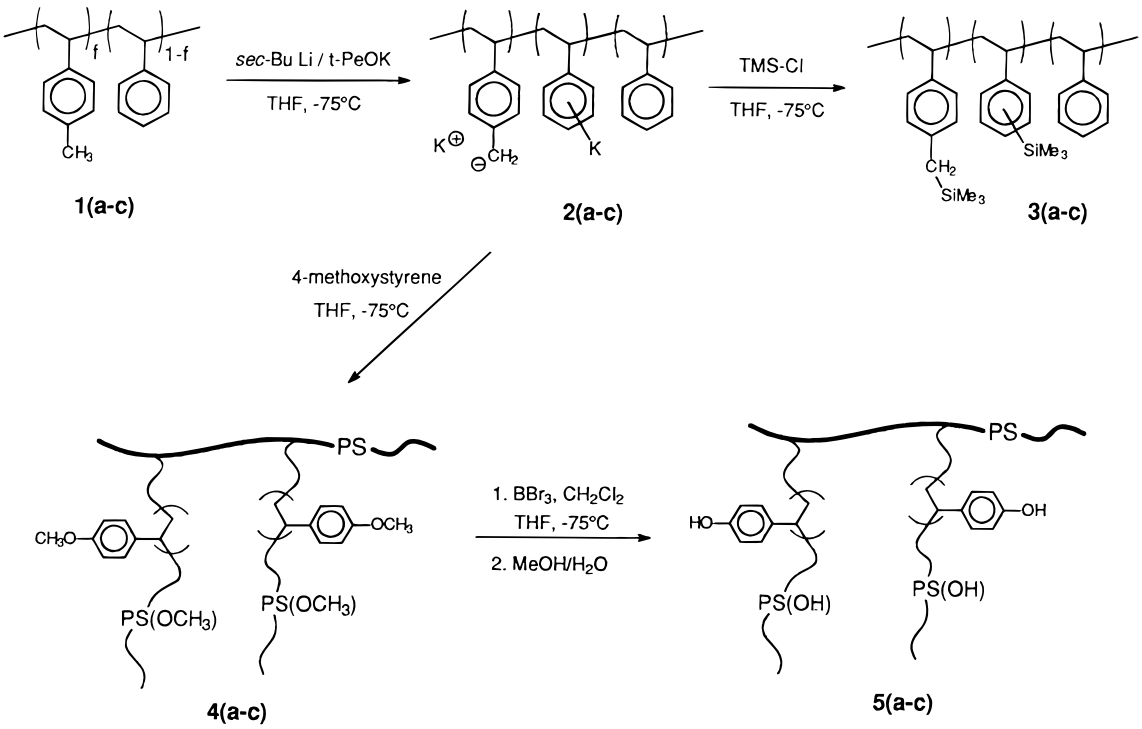

copolymers with different average spacings between grafting points and (ii) control the average number of grafted arms per polymer backbone. Conventional radical polymerization initiated by dicumyl peroxide was useful for the preparation of copolymers **1a** and **1b** having a broad range of molecular weights (Table 1). However, to determine the effects of the grafting reaction itself on the molecular weight distribution, a relatively monodisperse random copolymer was necessary. The preparation of random copolymers via living anionic polymerization can be difficult because monomers typically have very different reactivities toward the propagating anionic chain end. In our specific case, the targets were styrene/4-methylstyrene random copolymers. Since 4-methylstyrene is less reactive to an anionic initiator than styrene, copolymerization might lead to an undesirable blocklike structure. To avoid this problem, "living" radical polymerization was selected since the effect of the substituent on monomer incorporation is expected to be less drastic. By using a discrete "living" free-radical initiator developed by Hawker,[22] 1-phenyl-1-(2′,2′,6′,6′-tetramethyl-1′-piperidinyloxy)-ethane, copolymer **1c** was conveniently prepared with a polydispersity of 1.17 (Scheme 1). Deuterated random copolymers were prepared from styrene-d_8 in order to incorporate the deuterium tags required for FRES analysis of these copolymers in interfacial assemblies. Since styrene-d_8 contains 3 mol % remaining ^{1}H isotope, the composition determination of copolymers with low molar ratios of 4-methylstyrene by ^{1}H NMR was not complicated by significant overlap between the primary benzylic proton (2.25 ppm) and the backbone proton (1.2−1.8 ppm) resonances. Copolymers were prepared with low molar fractions of 4-methylstyrene in order to favor large spacings between graft points. By maximizing this spacing, the tendency for entanglement of the PS segments with bulk PS, which leads to enhanced interfacial strength, is increased.

Metalation has proven to be a useful synthetic tool for functionalizing otherwise unreactive polymers. In particular, polystyrene or polystyrene derivatives have been metalated using the complex of butyllithium and tetramethylethylenediamine. The resulting metalated polymers were then allowed to react with electrophiles to incorporate polar groups[27] or with monomers[28] to grow side chains. More recently, superbases prepared from the complex of alkyllithium and metal alkoxide (e.g. *sec*-butyllithium/potassium *tert*-pentoxide) have been shown by Lochmann and Fréchet to effectively metalate polystyrene[29] or copolymers of isobutylene and 4-methylstyrene.[30] The active superbase (SB) species is thought to be a complex between lithium alkoxide and alkylpotassium obtained in situ via metal exchange.[31] In general, the advantages of the alkylpotassium superbase over the alkyllithium/TMEDA system include higher reactivity and better selectivity.[29,30] For example, Lochmann has recently demonstrated[32] the selectivity of the SB by metalating poly(4-methylstyrene-*block*-styrene) predominantly at the primary benzylic sites (less than 1% ring metalation and no backbone metalation was detected). Given that the difference in acidity of the benzylic vs aromatic protons in that system is not very large ($\Delta pK_A < 2$), such a demonstration of superbase selectivity is impressive. We have adapted the use of the Lochmann-type superbase to the metalation of a random copolymer containing primary benzylic methyl groups in order to prepare a graft polymer by initiating anionic polymerization from multiple sites along the chain (Scheme 2). We chose to use the superbase prepared from *sec*-BuLi/t-PeOK in a 1:3 molar ratio because of the reactivity and selectivity demonstrated by the superbase prepared in such a fashion.[30] The conditions used for our metalation reactions, −75 °C in THF, were selected for their compatibility with the subsequent living anionic polymerization of 4-methoxystyrene initiated from the metalated copolymer (Scheme 2).

In general, the reactivity of SB is maximized with excess alkyllithium relative to the 4-methylstyrene substrate and a 3-fold molar excess of alkoxide relative

to alkyllithium. In our case, the former condition might lead to a serious problem for the subsequent graft polymerization reaction since any residual *sec*-butyllithium could compete with the polymeric initiator to produce undesired linear homopolymer mixed with the desired graft copolymer. However, at a polymerization temperature of −75 °C in THF, it might be expected that most of the monomer would be consumed via the grafting pathway since the propagating anion with potassium counterion is more highly dissociated than the corresponding lithium-coordinated anion. Nonetheless, to minimize the amount of homopolymer, SB was not used in excess; therefore, only partial metalation of the 4-methylstyrene units was carried out by design. As was the case in the preparation of the random copolymers, we designed a large average spacing between graft points by aiming for low degrees of metalation.

The degree of metalation of the copolymers was determined by ^{1}H NMR measurements on the aliquots quenched with chlorotrimethylsilane (**3a**−**c**, Scheme 2). The metalation efficiencies, denoted as f_K in Table 1, correlate the ratio of silylated sites observed to the amount of SB used. The mole percent of silylated sites was determined from integration data using the ratio of unreacted primary benzylic proton signals to silyl proton signals. The Ar−TMS and Ar−CH_2−TMS proton resonances are expected in the 0.1−0.2 ppm range and the 0 to −0.1 ppm range, respectively. For silylated poly(styrene-*co*-4-methylstyrene), **3a**−**c**, no proton resonances were observed upfield of 0 ppm, suggesting that metalation did not occur at the primary benzylic sites under these conditions. Interestingly, a peak at 0.09 ppm suggested that ring metalation had occurred instead. The calculated efficiency of the ring metalation was relatively low (40%). This is not unexpected in view of Lochmann's results with poly(styrene-*block*-4-methylstyrene) for which 2.0 mol equiv of SB relative to 4-methylstyrene units is needed to achieve complete metalation (>95%) at the primary benzylic position. Consequently, the metalation efficiencies of the two studies are comparable. Although the copolymer may actually be metalated at aromatic rather than benzylic sites, the process is nevertheless useful to prepare graft copolymers by polymerization from the metalated sites located along the polymer chain.

Graft Polymerization from Metalated Copolymer. Since the graft polymerization is designed to proceed by an anionic mechanism, a suitably protected monomer must be used in order to obtain poly(4-hydroxystyrene) grafts. The preparation of poly(4-hydroxystyrene) via anionic polymerization has been demonstrated using *tert*-butyldimethylsilyl-protected hydroxystyrene.[33] 4-Methoxystyrene is an attractive alternative to this silylated monomer. Its anionic polymerization has been described previously[34] and an analogous polymer, poly(4-*tert*-butoxystyrene), has been successfully deprotected[35] by reaction with a strong acid to afford poly(4-hydroxystyrene). Therefore, we focused on the polymerization of 4-methoxystyrene as a new, convenient route for the anionic preparation of poly(4-hydroxystyrene) grafts.

The polymerization of 4-methoxystyrene using the metalated poly(styrene-*co*-4-methylstyrene), **2**, was found to proceed to completion at −75 °C in THF after 2 h. For our interfacial studies of the copolymers, relatively short blocks of poly(4-hydroxystyrene) were desired ($N_{PS(OH)} < 100$). Therefore, the polymerizations of

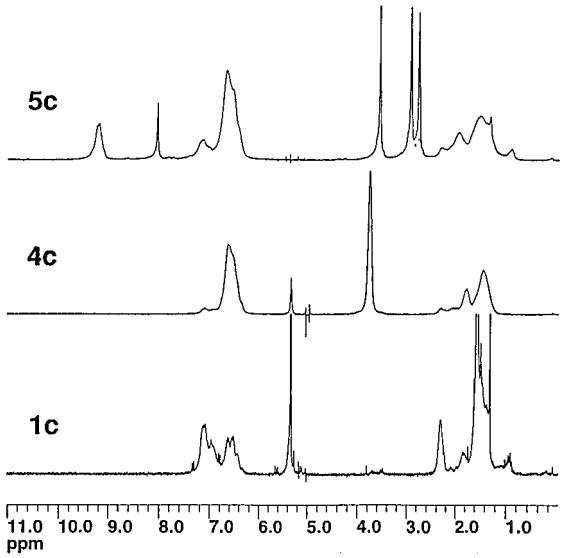

Figure 1. ^{1}H NMR of poly(styrene-d_8-*co*-4-methylstyrene), **1c**, in CD_2Cl_2; poly(styrene-d_8-*graft*-4-methoxystyrene), **4c**, in CD_2Cl_2; poly(styrene-d_8-*graft*-4-hydroxystyrene), **5c**, in DMF-d_7.

4-methoxystyrene were not carried to high molecular weight. The graft copolymerization results from the metalation route are summarized in Table 1. The SEC data confirm the presence of a unimodal product, free of any methoxystyrene homopolymer or random copolymer starting material. In each case, only a slight broadening of the molecular weight distribution is observed. By comparing the ^{1}H NMR of random copolymer **1c** with graft copolymer **4c** (Figure 1), the introduction of poly(4-methoxystyrene) grafts is evident as confirmed by the resonance at 3.8 ppm in addition to the enhanced resonance at 6.5 ppm. Since the starting copolymer is composed predominantly of styrene-d_8, the peaks from poly(4-methoxystyrene) are large in comparison.

Cleavage of the methoxy protecting groups of the poly(styrene-*graft*-4-methoxystyrene) copolymers was carried out quantitatively using boron tribromide. The ^{1}H NMR of **5c** in Figure 1 shows the complete loss of the methoxy protons at 3.8 ppm,[36] while the phenolic proton resonance is seen at 9.2 ppm. The quantitative nature of the cleavage to form poly(4-hydroxystyrene) is also observed under conditions similar to those of a poly(4-methoxystyrene) homopolymer prepared by conventional radical polymerization. To ascertain the effect of the deprotection conditions on the graft copolymer structure, **5c** was allowed to react with acetic anhydride to afford the corresponding acetate-protected copolymer. Protection of the phenolic groups is required prior to characterization of the copolymer by SEC in THF to avoid interactions with the columns. The relative molecular weight characteristics of the acetate-protected copolymer (M_n = 113 100, M_w/M_n = 1.45) is comparable to that of **4c** (M_n = 116 000, M_w/M_n = 1.32). Furthermore, there is no evidence for the formation of lower molecular weight side products that would arise from copolymer degradation.

Preparation of Graft Copolymers via ATRP. The ability of benzylic halides, such as 1-chloro-1-phenylethane, to initiate well-controlled, linear polymerization in the presence of copper(I) halide has been demonstrated previously.[37] By incorporating benzylic chloride pendent groups into the copolymer, atom-transfer radical polymerization of styrene initiated directly from the

Scheme 3

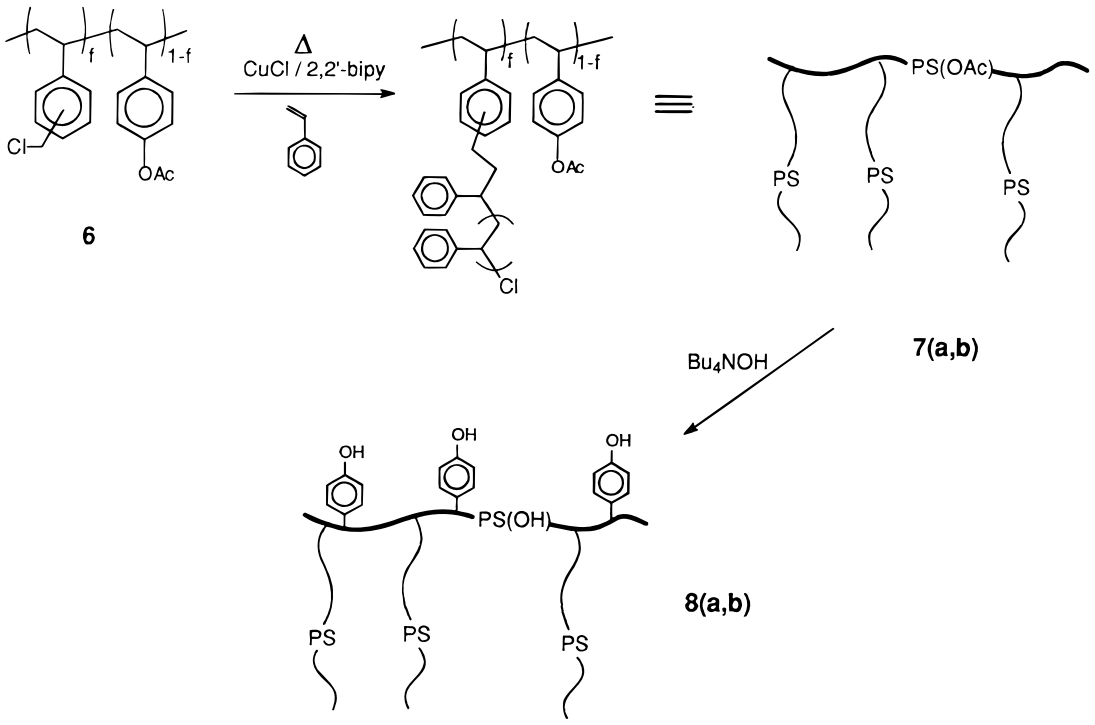

copolymer chain is possible. The starting macroinitiator copolymer **6** (Scheme 3) was prepared for use as a polymeric "living" radical initiator with multiple initiating sites along the copolymer chain. The preparation of **6** was carried out by TEMPO-mediated "living" radical copolymerization of vinylbenzyl chloride and 4-acetoxystyrene using the discrete initiator[22] shown in Scheme 1. Again, a copolymer with relatively low polydispersity (M_w/M_n = 1.14) was obtained (Table 2). 4-Acetoxystyrene was chosen as the comonomer to facilitate subsequent deprotection once the graft polymerization of styrene was completed, thereby leading to a copolymer with a poly(4-hydroxystyrene) main chain and polystyrene grafts (Scheme 3). The grafting polymerizations were carried out at 110 °C since the reactivity of the TEMPO end group is low compared to the activated benzyl chloride under these conditions. The graft polymerizations proceeded with moderate conversions of styrene (**7a**) and styrene-d_8 (**7b**), and the measured polydispersities were higher than expected for a living polymerization (Table 2). Deprotection of the phenolic groups of **7a,b** was carried out quantitatively at room temperature using tetrabutylammonium hydroxide to yield graft copolymers **8a,b** (Scheme 3). FTIR spectra confirmed that conversion was complete as evidenced by the loss of the carbonyl absorption (1765 cm^{-1}) and the appearance of a broad absorption in the 3300−3500 cm^{-1} region. ^1H NMR spectra were also consistent with the deprotected structures.

Preparation of Alternating Block Copolymers. The methods of living anionic polymerization to prepare block copolymers generally involve the sequential addition of monomers in the order of increasing reactivity to achieve clean crossover reactions and, therefore, monodisperse copolymers. Consequently, formation of alternating multiblock copolymers is limited to monomer pairs with very similar reactivities such as styrene/butadiene initiated by alkyllithium. Alternating block copolymers can also be prepared through the coupling of two telechelic homopolymer chains. However, this method generally does not afford well-defined and pure products. By using a "living" radical polymerization method, the choice of monomers can be expanded since the differences in reactivity toward a radical are frequently less critical. Furthermore, unlike living anionic or cationic reactions, many functional groups can be tolerated under "living" radical conditions. Recently, Nakagawa et al.[38] has reported the preparation of telechelic polystyrenes using bifunctional ATRP initiators, such as α,α′-dichloroxylene activated by the CuCl/2,2′-dipyridine complex. Extending this approach, a total of only three sequential polymerizations must be carried out in order to obtain an alternating pentablock structure (Scheme 4). Therefore, sequential atom-transfer radical polymerizations from a bifunctional initiator were used as described below to prepare the following series: polystyrene, poly(4-acetoxystyrene-*block*-styrene-*block*-4-acetoxystyrene), poly(styrene-*block*-4-acetoxystyrene-*block*-styrene-*block*-4-acetoxystyrene-*block*-styrene) (Scheme 4). Since 4-hydroxystyrene is not ideally suited for free-radical polymerizations, 4-acetoxystyrene was used as its protected equivalent. [(*tert*-Butoxycarbonyl)oxy]styrene,[39] used for the preparation of poly(styrene-*co*-4-hydroxystyrene) random copolymers,[21] was found to be unstable at the high temperature required for ATRP. Since our results with analogous random copolymers demonstrated the need for only small amounts of 4-hydroxystyrene relative to styrene in the copolymer,[21] block copolymers with short 4-acetoxystyrene blocks were considered optimal for this investigation.

The poly(styrene-d_8) macroinitiator, **9a**, was prepared in good conversions (85−90%) with a fairly narrow molecular weight distribution, consistent with a living polymerization mechanism (Table 3). The deuterium-labeled polymer is necessary for characterization by forward recoil spectrometry (FRES) but also simplifies some conventional characterization techniques. For instance, the ^1H NMR spectrum of the perdeuterated polystyrene clearly shows the expected benzylic meth-

Scheme 4

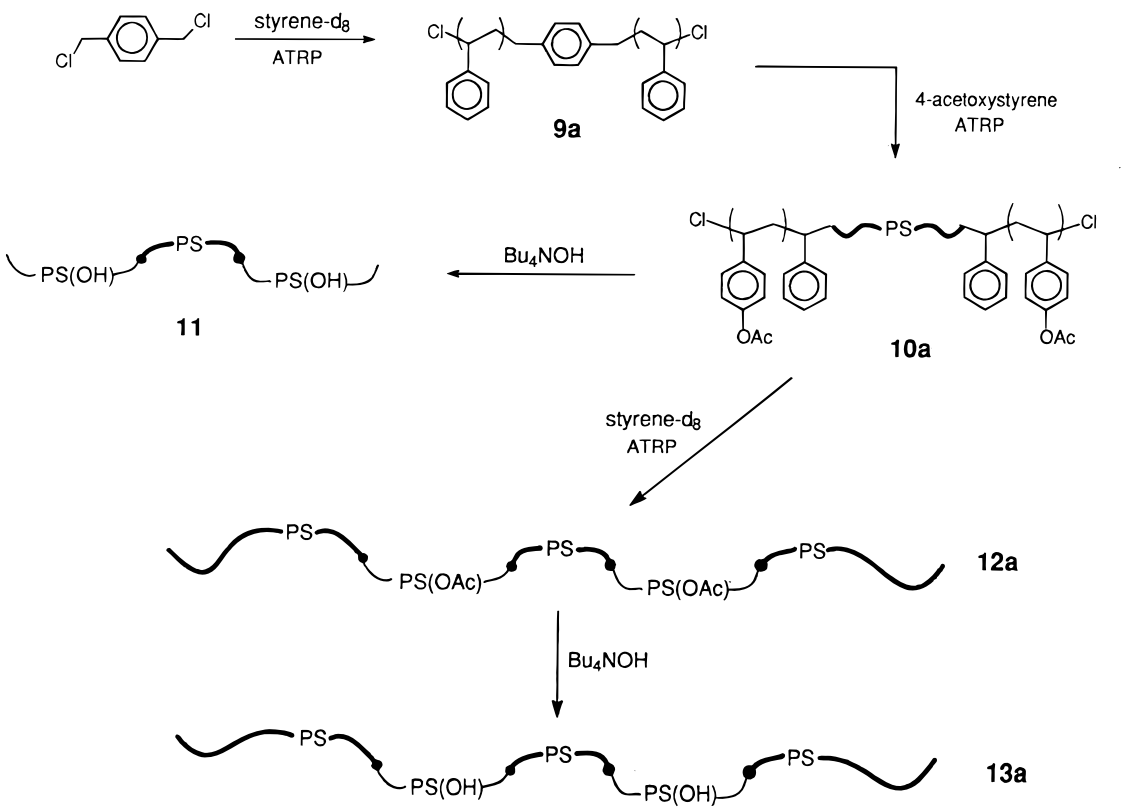

Table 3. Alternating Styrene−4-Acetoxystyrene Block Copolymers via ATRP

copolymer	% conv	$M_{n,calc}$[a] ($\times 10^3$)	M_n ($\times 10^3$)	M_w/M_n	P_n
9a	87	26.6	26.1[b]	1.22	252
10a	50	31.1	35.5[c]	1.27	29−252−29
12a	85	108.9	185.0[c]	2.31	400−29−252−29−400
9b	83	25.2	28.5[b]	1.31	276
10b	52	40.1	41.0[c]	1.31	46−276−46
12b	80	100.1	71.5[c]	1.77	316−46−276−46−316

[a] Calculated using M_n = MW × (M/I) × conversion, where MW denotes the monomer molecular weight and M/I denotes the monomer:initiator molar ratio. [b] Determined by SEC with polystyrene calibration. [c] Calculated from the SEC data of **9** and the NMR data of **10** or **12.**

ylene protons from the incorporation of the xylene initiator into the polymer backbone. Given the relatively controlled "living" polymerization process used, it is assumed that the polymer obtained is symmetrical about its initiating moiety.

Polymer **9a** was then used to initiate the polymerization of 4-acetoxystyrene to afford the triblock copolymer **10a**. Since the polymerization of 4-acetoxystyrene generally did not go to complete conversion (50−60%), excess monomer was used to achieve desirable block lengths. The difference in polymerizability of the two monomers may be due to the inherent differences in radical stability. The triblock copolymer was deprotected as described below to yield **11a**, poly(4-hydroxystyrene-*block*-styrene-d_8-*block*-4-hydroxystyrene).

Finally, **10a** was used as a polymeric initiator for the second polymerization of styrene-d_8. Surprisingly, the monomer conversion was very high (85−90%). However, characterization of the pentablock copolymer **12a** by SEC showed a broad but unimodal peak. Preparation of the corresponding ^{1}H-isotope styrene pentablock copolymer was carried out in an analogous manner to afford **9b**, **10b**, **12b**, and **13b** (Table 3). Deprotection of the triblock and pentablock copolymers using tetrabutylammonium hydroxide was quantitative in all cases.

Fracture Toughness Measurements. The 4-hydroxystyrene graft copolymers used for the interfacial strengthening study are summarized in Table 4. The fracture toughness of the PVP/PS interface as a function of the layer thickness and areal chain density of graft copolymer, **5b**, is shown in Figure 2a. Very little strengthening is seen at any thickness, and examination of the fracture surfaces indicates that all the deuterated polystyrene, dPS, from the copolymer is on the polystyrene side of the interface after fracture (Figure 2b). Therefore, pull-out of the poly(4-hydroxystyrene), PS(OH), blocks from the PVP side is the most likely failure mechanism. Other possible mechanisms which would be consistent with the deuterium distribution involve scission of the graft copolymer either at the backbone−arm junction or within the PS(OH) arm. These mechanisms seem less plausible since there is no compelling reason for the copolymer to always break at the backbone−arm junction or in the PS(OH) block and never experience breakage in the PS backbone. Clearly, if chain scission were involved, a fraction of the deuterium would be expected on the PVP surface. Therefore, the PS(OH) block which is 18 units on average (5 mol %) is too short to be sufficiently anchored in the PVP bulk phase.

As was made clear in the case of the PS−PS(OH) random copolymer, a low degree of 4-hydroxystyrene incorporation appears to be necessary for optimum interfacial strengthening.[21] In fact, random copolymers containing 6.6 mol % 4-hydroxystyrene were shown to be so miscible with the PVP bulk that little strengthening was observed. A comparison between graft copolymer **5b** and the random copolymer immediately brings

Table 4. Styrene/4-Hydroxystyrene Graft and Block Copolymers Used as Interfacial Reinforcers at the PS/PVP Interface

copolymer	M_w/M_n	P_n[a] graft arm	P_n[a] arm spacing	arms/chain	P_n[b] (copolymer)	mol % 4-HS[c]
5b	1.79	18	370	9	3492	5
5c	1.32	75	230	3.5	1068	21
8a	1.77	197	58	2.4	612	27
8b	1.63	365	58	2.4	1015	14
13a	2.31[c]	400−29−252−29−400			1110	5
11	1.27	29−252−29			310	19

[a] Determined from ^{1}H NMR integration. [b] Calculated from the SEC of the precursor and the NMR of the graft or block copolymer. [c] 4-HS: 4-hydroxystyrene.

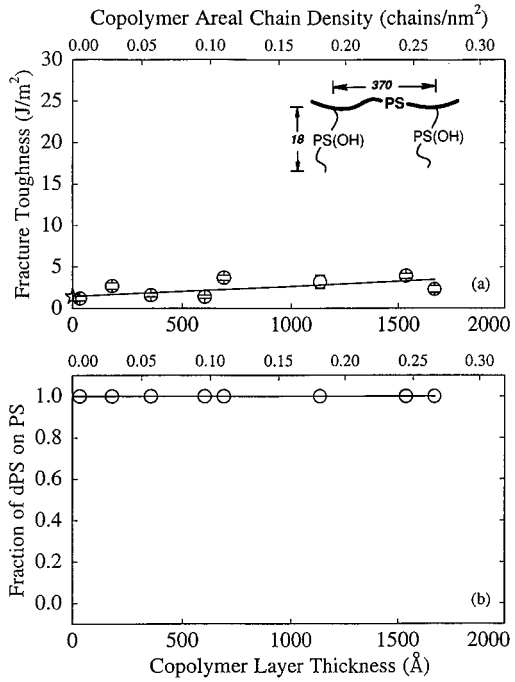

Figure 2. (a) Fracture toughness and (b) fraction of deuterated polystyrene, dPS, on the polystyrene side of the interface after fracture plotted as a function of the **5b** copolymer layer thickness and areal chain density.

to light some of the differences in the behavior between the graft copolymers and random copolymers with similar degrees of functionality. In the random copolymer, incorporation of only 3% H-bonding moieties affords optimum strengthening, while 5% incorporation clearly is not sufficient to prevent chain pull-out with the graft copolymer.

The strengthening behavior for a second graft copolymer with longer PS(OH) arms, **5c**, is shown in Figure 3a. Here, several salient features are observed. While the reinforced interface is sufficiently strong to form a visible craze, the fracture toughness exhibits a transition near $t^* = 300$ Å ($\Sigma^* = 0.17$ chains/nm^2). At higher thickness a maximum of 18 J/m^2 ($t_{max} = 500$ Å) is attained, and then a decrease to a constant value of 8 J/m^2 is observed. This critical thickness (areal chain density), t^* (Σ^*), is defined as the value for the onset of a transition from chain scission to crazing in the fracture mechanism and is reflected in the abrupt change in the deuterium distribution after fracture (Figure 3b).

Similar trends in interfacial strengthening were observed in earlier studies with symmetric PS−PVP diblocks[4] and with PS−PMMA diblocks.[1] In the studies[2] with long diblock copolymers which undergo one scission per chain during fracture, the chain scission-to-crazing transition is seen at $\Sigma^* = 0.03$ chains/nm^2. Since the transition value is dependent only on the number of scissions per chain and not on the copolymer architecture, a reinforcing copolymer which causes a transition above 0.03 chains/nm^2 must have only a fraction of the chains breaking during fracture. Therefore, in the case of the fracture of interfaces reinforced with low areal chain densities of **5c**, at most 18% of the chains (0.03/0.17) undergo scission while the remaining portion fail by pull-out. Since the spacing between the poly(hydroxystyrene) arms which was 230 styrene units on average and the entanglement degree of polymerization of PS is $N_E \approx 173$, extensive entanglement among the graft copolymers is not expected.

Assuming that the PS(OH) graft arms are placed randomly along the main chain, it is possible to estimate the fraction of intergraft spacings with a given number of monomer units. Using a Carothers-type approach, the fraction of intergraft PS segments with a $P_n > N$ is given by

$$\sum_{i=N}^{864} x_i = \int_N^{864} (1 - f_K)^{i-1} (f_K)^i \, di \qquad (1)$$

where i denotes the degree of polymerization for a given PS segment, x_i is the fraction of PS segments of length i in between graft points, and f_K is the degree of metalation. The upper limit is chosen to be the overall degree of polymerization of the graft backbone (see Table 1). Since two types of PS segments exist in the graft copolymer, end-segments and mid-segments, two critical lengths[7] for interfacial reinforcement are evaluated, $P_n > 200$ and $P_n > 400$. Evaluated for $N = 200$ and $f_K = 0.004$, eq 1 yields the value of 24% for the fraction of PS segments with a degree of polymerization 200 or greater and located at a main-chain end (assuming 2 PS end-segments/chain). For $N = 400$, the calculated fraction of PS segments with a degree of polymerization 400 or greater is 17%. At this degree of polymerization, which is greater than $2N_E$, some strengthening as a result of entanglement with the PS bulk is expected. These estimated fractions of entangled PS segments are in reasonable agreement with the amount of chain scission deduced above from the scission-to-crazing transition (18%).

The fact that some chains undergo scission indicates that the PS(OH) block must be long enough to resist pull-out from the PVP side. Although the entanglement degree of polymerization, N_E, for PS(OH) was not experimentally determined, it is reasonable to assume a lower limit of $N_E \approx 173$, that of PS. However, in the case of PS(OH) in the PVP phase, entanglement is likely not a significant factor since $N_{PS(OH)} = 75$. Instead, two factors are jointly responsible for the observed resistance

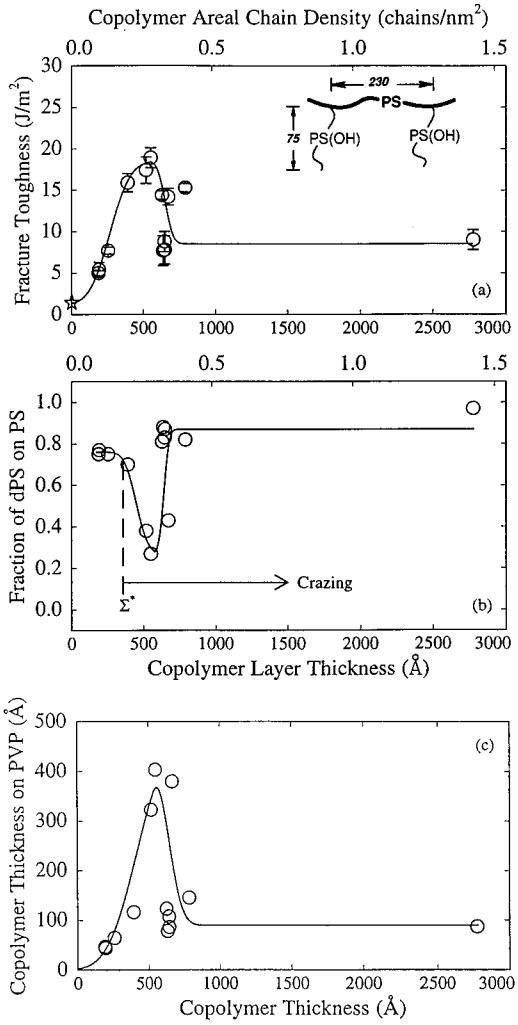

Figure 3. (a) Fracture toughness and (b) fraction of deuterated polystyrene, dPS, on the polystyrene side of the interface after fracture plotted as a function of the **5c** copolymer layer thickness and areal chain density. (c) Thickness of **5c** layer on the PVP side after fracture vs. total thickness of **5c** layer at the interface.

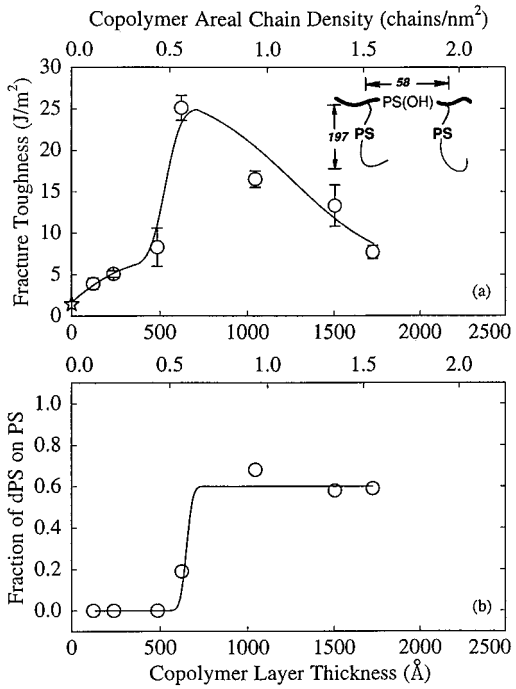

Figure 4. (a) Fracture toughness and (b) fraction of deuterated polystyrene, dPS, on the polystyrene side of the interface after fracture plotted as a function of the **8a** copolymer layer thickness and areal chain density.

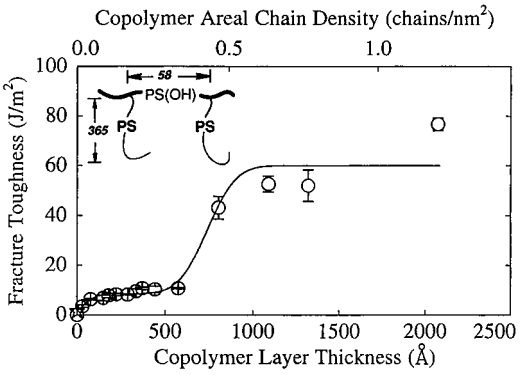

Figure 5. Fracture toughness plotted as a function of the **8b** copolymer layer thickness and areal chain density.

to chain pull-out: (i) the cumulative enthalpic gains resulting from H-bonding of the PS(OH)−PVP interactions ($\chi_{PS(OH)-PVP} = -0.28$)[20] and (ii) the enthalpic penalty of the PS−PS(OH) interactions ($\chi_{PS-PS(OH)} = 6$)[21] as the PS(OH) segments are pulled to the PS side.

Interestingly, the ^{2}H distribution data of **5c** exhibit a minimum as a function of copolymer areal chain density which correlates with the maximum in toughness. A better understanding of the fracture mechanism is facilitated by the representation of the copolymer thickness on the PVP side after fracture as a function of total copolymer thickness in Figure 3c. From this plot for $t < t_{max}$ ($t_{max} = 500$ Å) the formation of a single copolymer layer along the PVP/copolymer interface is suggested. When the interface fractures in this regime below t_{max}, the crack propagates between the copolymer and the PS homopolymer, leaving progressively more copolymer on the PVP side at larger thicknesses. After a complete lamellar layer is formed at $t = t_{max}$, fracture occurs between the complete lamella and the second developing lamella. After the complete formation of the second lamella ($t \approx 800$ Å), the fracture toughness reaches a saturation value since the formation of additional lamella does not change the locus of fracture.

The change in the locus of fracture from the copolymer/PS interface ($t < t_{max}$) to within the copolymer layer ($t > t_{max}$) results in the decrease in the fracture toughness. Since the locus of fracture remains constant in the regime above t_{max}, a constant copolymer layer thickness (100 Å) is observed on the PVP side in Figure 3c and the fraction of deuterium on the PS side (Figure 3b) approaches 1.0 in the high t limit. Although lamellar structures seem likely in light of the fracture data, the observation in the DSC trace of two glass transitions for **5c** corresponding to the PS segments ($T_{g1} = 104$ °C) and the PS(OH) segments ($T_{g2} = 194$ °C) suggests that the annealing temperature of the samples is not high enough to allow for motion of PS(OH) segments. Therefore, nonequilibrium microphase-separated structures are probably present and complicate the interpretation of the fracture data.

The results of **5b** and **5c** can be compared to those of graft copolymers **8a** and **8b** which have PS arms and a PS(OH) backbone (Figures 4 and 5). The toughness data for **8a** (Figure 4a) show a trend similar to that of **5c**, exhibiting an upturn beyond $t^* = 550$ Å ($\Sigma = 0.54$

chains/nm^2), followed by a maximum (G_C = 25 J/m^2, t_{max} = 700 Å) and then a decrease to 8 J/m^2. However, the distribution of copolymer **8a** on the fracture surfaces in Figure 4b suggests that the mechanism of fracture is different from that for **5c**. For $t < t^*$ (t^* = 550 Å, Σ^* = 0.54 chains/nm^2) the PS portion of the copolymer is observed predominantly (90%) on the PVP side which would be consistent with some chain scission of the graft copolymer. The onset of a transition in the copolymer ^{2}H distribution curve at t^* = 550 Å (Σ^* = 0.54 chains/nm^2) is followed by a plateau where an approximately 60%/40% distribution of copolymer exists on the PS/PVP surfaces, respectively.

The transition in ^{2}H distribution, which is evidence for a change in the failure mechanism, corresponds closely to the upturn in fracture toughness. However, according to the critical areal chain density, 0.54 chains/nm^2, only 5% (0.03/0.54) of the copolymer chains must be breaking during fracture. Furthermore, since the PS arms in **8a** are short (N_{PS} = 197), chain pull-out from the PS bulk would be expected to play a major role in the failure mechanism. A similar dependence of the ^{2}H distribution on areal chain density has been demonstrated for PS−PVP diblock[4] and PVP−PS−PVP triblock[7] copolymers with short PVP blocks ($N_{PVP} < N_{E,PVP}$) where a transition from pull-out to crazing was observed. Therefore, it is likely that a similar transition occurs for interfaces reinforced with graft copolymer, **8a**, given that pull-out is the dominant mechanism at low t, but beyond t^* craze formation is suggested by the high fracture toughness values and the visual observation of fracture surfaces.

In contrast to the previous studies, the observed maximum in the fracture toughness in Figure 4a is consistent with the formation of a lamellar layer as described above for **5c**. As a second lamellar layer of **8a** begins to form at $t > t_{max}$, the crack propagates between the lamellae where copolymer chains are poorly entangled, leaving 60% of the copolymer on the PS side. Since the failure mode of **8a** is predominantly pull-out, the locus of fracture is not the same as that in the case of **5c** in which chain scission is more prevalent.

The fracture toughening data for **8b** are shown in Figure 5. Since this copolymer was not deuterium-labeled, no copolymer distribution data are reported. Initially, the fracture toughness is observed to increase slowly with increasing copolymer thickness until a jump to almost 50 J/m^2 at t^* = 600 Å (Σ^* = 0.35 chains/nm^2) which suggests the formation of a craze. The occurrence of this transition at high areal chain density is consistent with a fracture mechanism of pull-out and some chain scission. It is not clear if lamellar structures can form in the case of **8b** which has only 14 mol % poly(4-hydroxystyrene). Ongoing studies of the interfacial morphology using TEM may reveal the nature of the strengthening more clearly. Regardless, the PS-rich domains in the microphase-separated structure must be entangled in order to impart significant reinforcement of the craze fibrils.

At this juncture, it is important to contrast the structures of **8b** and **8a** which differ in the length of their PS arms. If a "hairpin" configuration is assumed, the PS(OH) backbone is anchored to the PVP/copolymer layer interface while the PS entangles with other copolymer chains or with the PS homopolymer. In both cases the enthalpic interactions are able to sufficiently tether the PS(OH) backbone. Since copolymer **8b** has

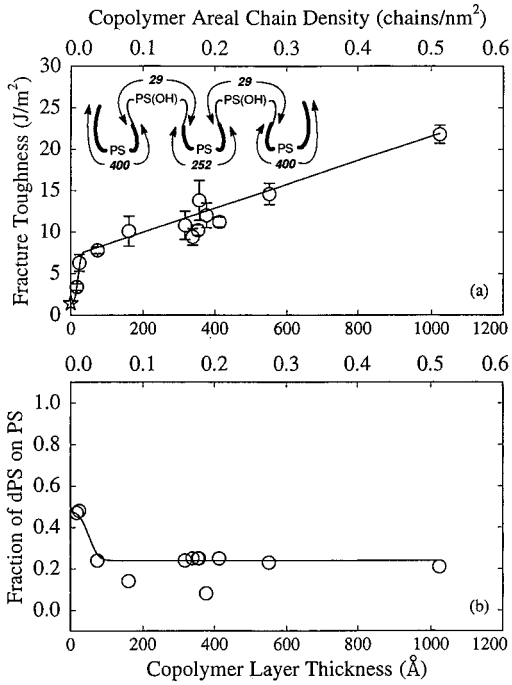

Figure 6. (a) Fracture toughness and (b) fraction of deuterated polystyrene, dPS, on the polystyrene side of the interface after fracture plotted as a function of the **13** copolymer layer thickness and areal chain density.

sufficiently long PS arms which more strongly reinforce the craze fibrils, the interface has a higher fracture toughness in the crazing regime. In contrast, the short PS arms of **8a** afford poorer entanglement and therefore only a narrow craze forms which dissipates considerably less energy.

For pentablock copolymer **13a** the dependence of interfacial toughness on layer thickness is shown in Figure 6a. The fracture toughness increases sharply at very low copolymer layer thickness and then continues to increase at a slower rate. The transition occurring at a value estimated near t^* = 30 Å (Σ^* = 0.016 chains/nm^2) is reflected in the copolymer distribution data in Figure 6b. Below t^* the PS blocks are distributed 50:50 on the fracture surfaces, but at higher thicknesses the distribution shifts to a ratio of approximately 25:75 on the PS and PVP surfaces. At low thicknesses ($t < t^*$) a significant amount of dPS is observed on the PVP side after fracture, which suggests that chain scission is not the sole failure mechanism. If chain scission were the only mechanism, a behavior similar to that observed by Dai et al. for long triblock copolymers[7] is expected in which 90% of the dPS was found on the PS side.

A comparison of the pentablock copolymer with its deprotected triblock precursor copolymer allows an evaluation of the effect of the outer PS blocks in **13a**. The fracture toughness is observed to rise must faster with increasing the areal chain density of the pentablock copolymer than in the case of the triblock copolymer shown in Figure 7a. The copolymer distribution data of **13a** suggest the presence of significant PS block entanglement with the bulk PS. In contrast, the interface reinforced with triblock copolymer, **11**, fails by pull-out of the PS middle block at all thicknesses (Figure 7b). The fact that PS undergoes chain pull-out instead of the PS(OH) chain is striking considering the respective lengths: N_{PS} = 252, $N_{PS(OH)}$ = 29. This

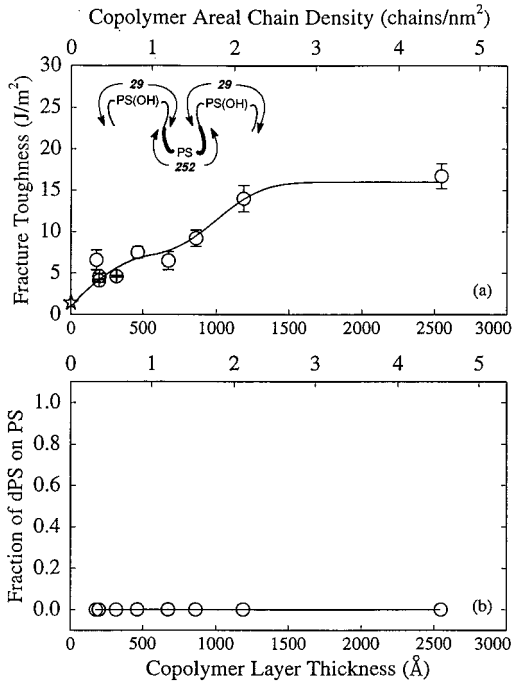

Figure 7. (a) Fracture toughness and (b) fraction of deuterated polystyrene, dPS, on the polystyrene side of the interface after fracture plotted as a function of the **11** copolymer layer thickness and areal chain density.

behavior of the triblock copolymer suggests that the middle block of **13a** also fails by pull-out from the PS side. If the middle block was not well-entangled, then the pentablock copolymer should behave as a triblock copolymer reinforcer at the interface. Dai et al. has shown that an interface reinforcement with triblock copolymer undergoes a scission-to-crazing transition at $\Sigma^* = 0.015$ chains/nm^2, which corresponds closely to the observed transition seen for the case of **13a**.

Conclusion

This study demonstrates the value of living radical polymerization for the preparation of copolymers with a variety of interesting architectures. Easy access to functionalized block and graft structures, formerly almost exclusively accessible through a demanding anionic technique, allows their evaluation in interfacial strengthening studies. The presence of block and graft copolymers based on polystyrene and poly(4-hydroxystyrene) at the PS/PVP interface can significantly enhance the interfacial fracture toughness depending on the lengths of the PS and PS(OH) segments. The PS(OH) segment length was surprisingly effective at anchoring into the PVP phase even at low degrees of polymerization, suggesting that hydrogen bonds contribute significantly to the pull-out resistance. Since these amphiphilic copolymers tend to form microphase-separated structures, the most effective copolymer reinforcers create strong phase domains in addition to strong connectors between phase domains. For a further understanding of the strengthening potential of these types of copolymers, studies on the kinetics of the microphase formation would be useful.

While some of the block and graft architectures reported herein afford strengthening of the PS−PVP interface, their performance still appears to be inferior to that of the very simple random copolymer structures we have recently described. Thus, it may not be necessary to prepare block and graft structures in cases where strengthening through the formation of strong H-bonds is possible. Alternatively, by further tuning the molecular weight characteristics of functionalized graft and block copolymers, the development of a new class of interfacial reinforcers may be viable.

Acknowledgment. Financial support of the Cornell Materials Science Center under a grant from the National Science Foundation (DMR 9121654 and 9641291) is gratefully acknowledged. We also appreciate the use of the Ion Beam Analysis Central Facility of the Materials Science Center and the invaluable assistance of P. Revesz and N. Szabo of this facility.

References and Notes

(1) Brown, H. R.; Deline, V. R.; Green, P. F. *Nature* **1989**, *341*, 221. Brown, H. R. *Macromolecules* **1989**, *22*, 2859.
(2) Creton, C. F.; Kramer, E. J.; Hui, C. Y.; Brown, H. R. *Macromolecules* **1992**, *25*, 3075.
(3) Char, K.; Brown, H. R.; Deline, V. R. Deline, *Macromolecules* **1993**, *26*, 4164.
(4) Washiyama, J.; Creton, C. F.; Kramer, E. J.; Xiao, F.; Hui, C. Y. *Macromolecules* **1993**, *26*, 6011.
(5) Creton, C. F.; Brown, H. R.; Deline, V. R. *Macromolecules* **1994**, *27*, 1774.
(6) Washiyama, J.; Kramer, E. J.; Creton, C. F.; Hui, C.-Y. *Macromolecules* **1994**, *27*, 2019.
(7) Dai, C.-A.; Jandt, K. D.; Iyengar, D. R.; Slack, N. L.; Dai, K. H.; Davidson, W. B.; Kramer, E. J.; Hui, C.-Y. *Macromolecules* **1997**, *30*, 549.
(8) Boucher, E.; Folkers, J. P.; Hervet, H.; Léger, L.; Creton, C. *Macromolecules* **1996**, *29*, 774.
(9) Brown, H. R.; Char, K.; Deline, V. R.; Green, P. F. *Macromolecules* **1993**, *26*, 4155.
(10) Dai, C. A.; Dair, B. J.; Dai, K. H.; Ober, C. K.; Kramer, E. J.; Hui, C.-Y.; Jelinski, L. W. *Phys. Rev. Lett.* **1994**, *73* (18), 2472. Dai, C.-A.; Osuji, C. O.; Jandt, K. D.; Dair, B. J.; Ober, C. K.; Kramer, E. J.; Hui, C.-Y. *Macromolecules* **1997**, submitted for publication.
(11) Kulasekere, R.; Kaiser, H.; Ankner, J. F.; Russell, T. P.; Brown, H. R.; Hawker, C. J.; Mayes, A. M. *Macromolecules* **1996**, *29*, 5493.
(12) Winey, K. I.; Berba, M. L.; Galvin, M. E. *Macromolecules* **1996**, *29*, 2868.
(13) Guo, L.; Rafailovich, M. H.; Sokolov, J.; Peiffer, D.; Schwarz, S. A.; Eisenberg, A. *Bull. Am. Phys. Soc.* **1996**, *41* (1), 318.
(14) Paul, D. R., Newman, S., Eds. *Polymer Blends*; Academic Press: New York, 1978; Vol. 2, p 35.
(15) Gersappe, D.; Irvine, D.; Balazs, A. C.; Liu, Y.; Sokolov, J.; Rafailovich, M.; Schwarz, S.; Peiffer, D. G. *Science* **1994**, *265*, 1072.
(16) Lee, Y.; Char, K. *Macromolecules* **1994**, *27*, 2603.
(17) Norton, L. J.; Smigolova, V.; Pralle, M. V.; Hubenko, A.; Dai, K. H.; Kramer, E. J.; Hahn, S.; Berglund, C.; DeKoven, B. *Macromolecules* **1995**, *28*, 1999.
(18) Vivas de Meftahi, M.; Fréchet, J. M. J. *Polymer* **1988**, *29*, 477.
(19) Kato, T.; Fréchet, J. M. J. *J. Am. Chem. Soc.* **1989**, *111*, 8533. Kato, T.; Fréchet, J. M. J. *Macromolecules* **1989**, *22*, 3818.
(20) Dai, K. H.; Kramer, E. J.; Fréchet, J. M. J.; Wilson, P. G.; Moore, R. S.; Long, T. E. *Macromolecules* **1994**, *27*, 5187.
(21) Xu, Z.; Kramer, E. J.; Edgecombe, B. D.; Fréchet, J. M. J. *Macromolecules* **1997**, submitted for publication.
(22) Hawker, C. J.; Barclay, G. C.; Orellano, A.; Dao, J.; Devonport, W. *Macromolecules* **1996**, *29* (16), 5245.
(23) Brown, H. R. *Macromolecules* **1989**, *22*, 2859
(24) Brown, H. R. *Macromolecules* **1991**, *24*, 2752. Kausch, H. H. *Polymer Fracture*, 2nd ed.; Springer-Verlag: Berlin, 1987. Odell, J. A.; Keller, A. *J. Polym. Sci., Polym. Phys. Ed.* **1985**, *24*, 1889.
(25) Xiao, F.; Hui, C.-Y.; Washiyama, J.; Kramer, E. J. *Macromolecules* **1994**, *27*, 4382.
(26) Doyle, B. L.; Peercy, P. S. *Appl. Phys. Lett.* **1979**, *34*, 811. Mills, P. J.; Green, P. F.; Palmstrøm, C. J.; Mayer, J. W.; Kramer, E. J. *Appl. Phys. Lett.* **1984**, *45*, 957.

(27) Chalk, A. J. *J. Polym. Sci., Part B* **1968**, *6*, 649. Farrall, M. J.; Fréchet, J. M. J. *J. Org. Chem.* **1976**, *41*, 3877.
(28) Plate, N. A.; Yampol'skaya, M. A.; Davydova, S. L.; Kargin, V. A. *J. Polym. Sci. Part C* **1969**, *22*, 547. Kennedy, J. P.; Nakao, M. *J. Appl. Polym. Sci., Appl. Polym. Symp.* **1977**, *30*, 73. Harris, J. F.; Sharkey, W. H. *Macromolecules* **1986**, *19*, 2903.
(29) Lochmann, L.; Fréchet, J. M. J. *Macromolecules* **1996**, *29* (5), 1767.
(30) Steinke, J. H. G.; Haque, S. A.; Fréchet, J. M. J.; Wang, H. C. *Macromolecules* **1996**, *29* (19), 6081.
(31) Lochmann, L.; Trekoval, J. *J. Organomet. Chem.* **1987**, *326*, 1.
(32) Lochmann, L.; Janat, M.; Holler, P.; Tuzar, Z.; Kratochvil, P. *Macromolecules* **1996**, *29*, 8092.
(33) Hirai, A.; Yamaguchi, K.; Takenaka, K.; Suzuki, K.; Nakahama, S. *Makromol. Chem., Rapid Commun.* **1982**, *3*, 941.
(34) Shima, M.; Bhattacharvya, D. N.; Smid, J.; Szwarc, M. *J. Am. Chem. Soc.* **1963**, *8*, 1306. Geerts, J.; Van Beylen, M.; Smets, G. *J. Polym. Sci., Polym. Chem. Ed.* **1969**, *7*, 2859.
(35) Conlon, D. A.; Crivello, J. V.; Lee, J. L.; O'Brien, M. J. *Macromolecules* **1989**, *22*, 509.
(36) The peak at 3.6 ppm is due to adventitious water in the DMF-d_7 NMR solvent.
(37) Wang, J.-S.; Matyjaszewski, K. *J. Am. Chem. Soc.* **1995**, *117*, 5614.
(38) Nakagawa, Y.; Gaynor, S. G.; Matyjaszewski, K. *Polym. Prepr. (Am. Chem. Soc., Div. Polym. Chem.)* **1996**, *37* (1), 577.
(39) Fréchet, J. M. J.; Eichler, E.; Willson, C. G.; Ito, H. *Polymer* **1983**, *24*, 995.

MA970832Q